Monitoring methane emissions from space

Thibaud Ehret

Thanks to

Elyes Ouerghi
Gabriele Facciolo
Enric Meinhardt
Jean-Michel Morel

Aurélien de Truchis
Alexis Groshenry
Carlo de Franchis
Clément Giron

And many others!

Global warming is linked to methane

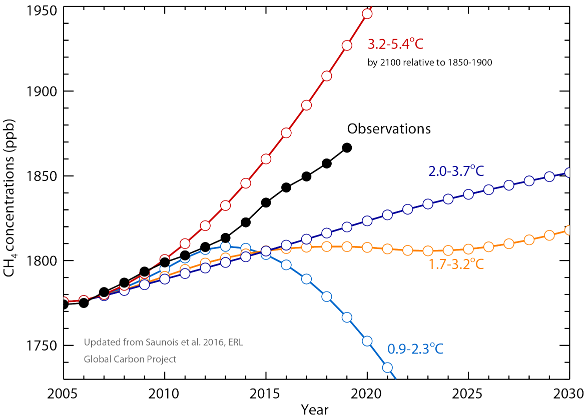

Figure 1: Evolution of methane concentration according to different scenarios of global warming. (source[1])

[1] Saunois et al. "The global methane budget 2000–2017". In: *Earth system science data* (2020).

Methane budget

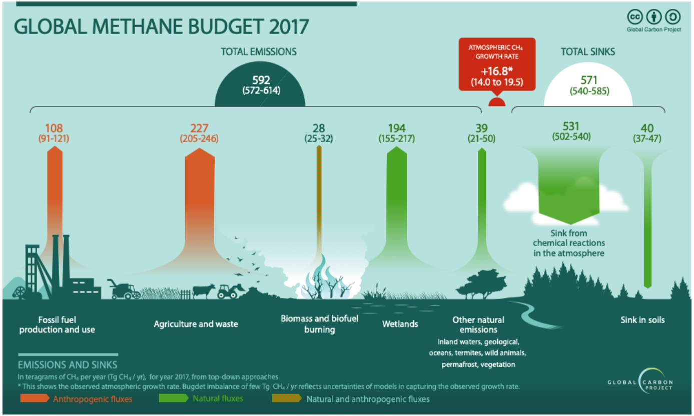

Figure 2: The global methane budget for 2017. (source[2]).

[2] Jackson et al. “Increasing anthropogenic methane emissions arise equally from agricultural and fossil fuel sources”. In: *Environmental Research Letters* (2020).

Who's interested by emissions monitoring?

Oil and gas operators

- Monitoring assets.

Institutions

- Verify that legislations are properly followed (e.g. Permian basin, US).
- Can be used to propose new legislations (e.g. "is natural gas a green energy?").

Scientists

- Inversion models require precise priors.

How to monitor emissions? (on-site or airborne campaigns)

How to monitor emissions? (TROPOMI)

- Launched in 2017
- Air quality and climate monitoring
- Dedicated methane product
- Data only available where the atmospheric inversion was successful

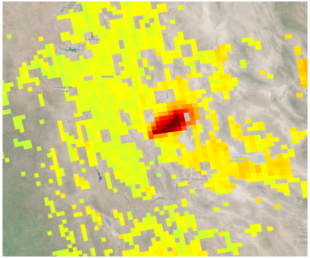

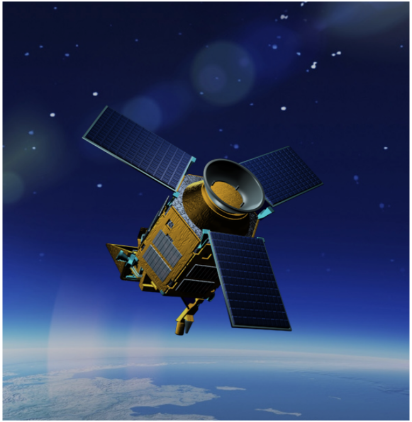

(Source: ESA)

Satellites for methane emission monitoring

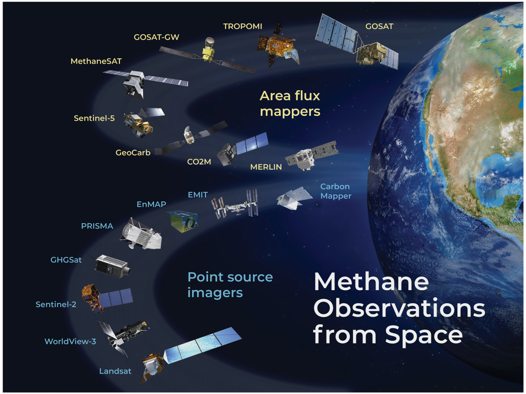

Figure 3: (Some) satellite used for methane observation from space. (Source[3])

[3] Jacob et al. "Quantifying methane emissions from the global scale down to point sources using satellite observations of atmospheric methane". In: *Atmospheric Chemistry and Physics* (2022).

How do satellites see methane?

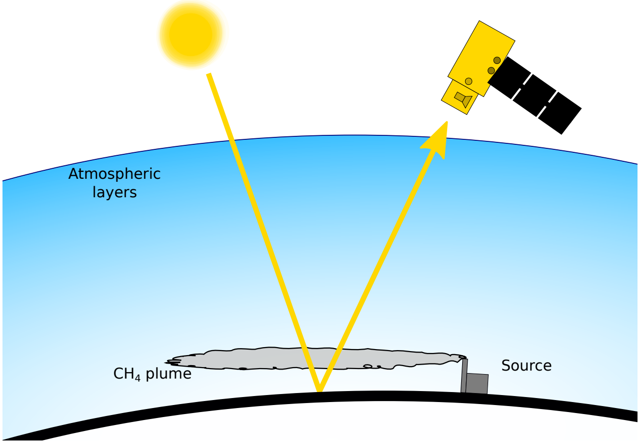

Figure 4: Observation model for a satellite with a passive sensor.

Absorption model

Beer-Lamber law for a wavelength λ:

$$I(\lambda) = I_0(\lambda)e^{-\sum_{i=0}^{\ell} A_i(\lambda)L_i}. \tag{1}$$

Notations:

- ℓ gases;
- Each gas can be caracterized by its absorption coefficient A and its quantity L;

A zoom on two categories: hyperspectral and multispectral

Mission	Spatial resolution	Spectral resolution	Spatial coverage	Temporal coverage	Cost
Airborne campaign (e.g. AVIRIS-NG)	High (0.3m to 4m)	high (425 bands)	Low (tasking)	Low (tasking)	High
Sentinel-5P	Low ($\sim$7km)	High (2600 bands)	High (global coverage)	High (daily)	Low
PRISMA	High (30m)	High (239 bands)	Low (tasking)	Low (tasking)	Low
Sentinel-2	High (10m to 20m)	Low (13 bands)	High (global coverage)	High ($\sim$5 days)	Low

Outline

1 - Hyperspectral monitoring

2 - Multispectral monitoring

3 - Validation

4 - Perspectives

Outline

1 - Hyperspectral monitoring

2 - Multispectral monitoring

3 - Validation

4 - Perspectives

Matched filter: an anomaly detection framework

- Let $x \in \mathbb{R}^d$ be an observed pixel with d spectral samples.
- In absence of anomaly, we assume that the image follows a multivariate normal distribution $\mathcal{N}(\mu, \Sigma)$.
- We denote by K_{CH4} the absorption spectrum of methane.
- Linear approximation of Beer-Lambert law for weak plumes $x \approx z - \alpha K_{\mathrm{CH4}} z$.
- To have a constant anomaly direction it is a widely common practice[4] replace z by μ (i.e. $x \approx z - \alpha K_{\mathrm{CH4}} \mu$).
- The best linear detector is the matched filter[5]

$$\mathcal{D}_{MF}(x) = \frac{\mathbf{t}^T \Sigma^{-1}(x - \mu)}{\mathbf{t}^T \Sigma^{-1} \mathbf{t}} \qquad \text{with} \qquad \mathbf{t} = -\alpha K_{\mathrm{CH4}} \mu. \tag{2}$$

[4] Thompson et al. “Real-time remote detection and measurement for airborne imaging spectroscopy: a case study with methane”. In: *Atmospheric Measurement Techniques* (2015).

[5] Theiler and Wohlberg. “Detection of unknown gas-phase chemical plumes in hyperspectral imagery”. In: *Alg. and Tech. for Multispectral, Hyperspectral, and Ultraspectral Imagery*. 2013.

Matched filter: Geometric interpretation (in dimension 2)

In the whitened space

- $y = \Sigma^{-1/2}(x - \mu)$,
- $u = \frac{\Sigma^{-1/2}\mathbf{t}}{\mathbf{t}^T\Sigma^{-1}\mathbf{t}}$.

Match filter

$\mathcal{D}_{WMF}(y) = y^T u$.

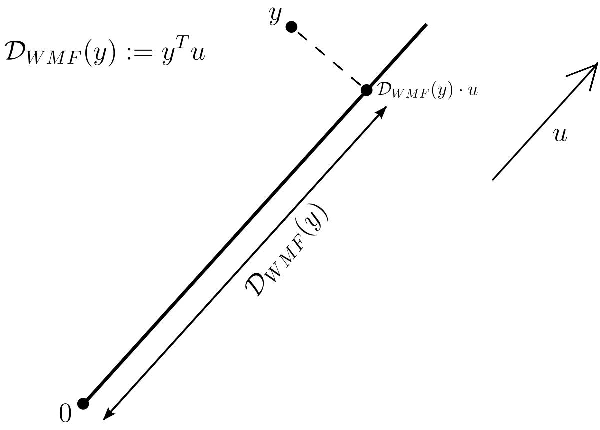

Figure 5: Geometric visualization of the matched filter.

Matched filter: removing non-methane anomalies

Adjusted filter[6]

$\mathcal{D}_{AMF}(x) = \frac{\mathcal{D}_{MF}(x)}{\sqrt{\mathcal{D}_{RX}(x)}}$

Reed-Xiaoli detector[7]

$\mathcal{D}_{RX}(x) = (\mathbf{x} - \mu)^{\mathrm{T}}\Sigma^{-1}(\mathbf{x} - \mu)$

Whitened space

In the whitened space we can write $\mathcal{D}_{RX}(x)$ as $\mathcal{D}_{WRX}(y) := y^T y$.

---

[6] Matteoli, Marco Diani, and Giovanni Corsini. "A tutorial overview of anomaly detection in hyperspectral images". In: *IEEE Aerospace and Electronic Systems Magazine* (2010).

[7] Irving S Reed and Xiaoli Yu. "Adaptive multiple-band CFAR detection of an optical pattern with unknown spectral distribution". In: *IEEE transactions on acoustics, speech, and signal processing* (1990).

Matched filter techniques: geometric interpretation

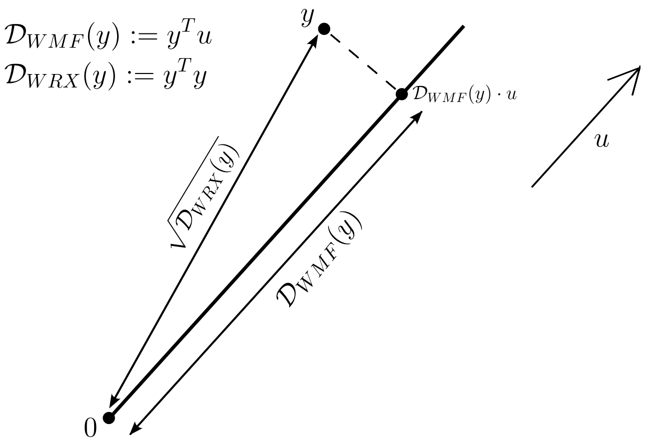

Figure 6: Geometric visualization of the matched filter.

Model Adjusted Matched Filter (MAMF)[8]

Model adjustment coefficient (whitened space)

$\mathcal{D}_{WMA}(y) := \|y - \mathcal{D}_{WMF}(y)u\|_2^2$

Model adjustment coefficient (original space)

$\mathcal{D}_{MA}(x) = \mathcal{D}_{RX}(x - \mathcal{D}_{MF}(x)t).$

Model Adjusted Matched Filter (MAMF)

$\mathcal{D}_{MAMF}(x) = \frac{\mathcal{D}_{MF}(x)}{\mathcal{D}_{MA}(x)^q}.$

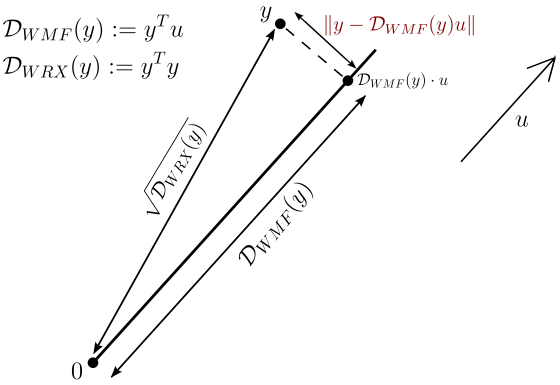

Figure 7: Geometric visualization of the matched filter.

[8] Ouerghi et al. "Model Adjusted Generalized Tests for methane plume detection on hyperspectral images". In: *WHISPERS*. IEEE. 2023.

Model adjustment: MAMF results

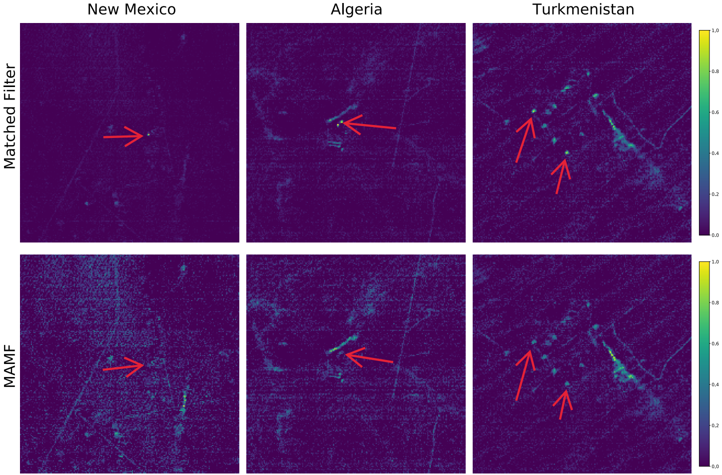

Figure 8: Visual comparison between the MF and the MAMF.

Model adjustment: a better separation of the distributions

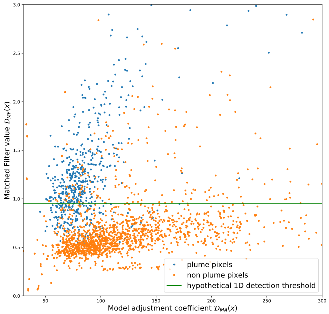

Figure 9: Pixel distribution with the MF.

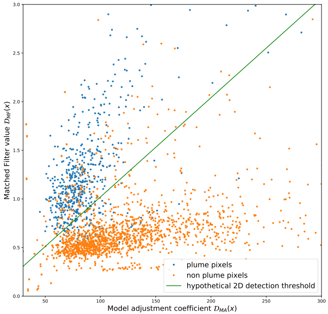

Figure 10: Pixel distribution with the MF and MA axes.

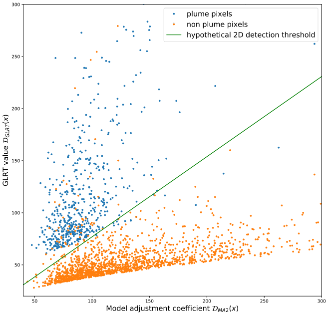

Figure 11: Pixel distribution with the GLRT and MA2 axes.

Model adjustment: numerical results

Detector	Recall	Precision	F1
ACE[9]	0.24	0.37	0.29
MF[10]	0.27	0.32	0.29
MAMF (ours)	0.39	0.56	0.46
GLRT	0.36	0.56	0.44
MAGLRT[11] (ours)	**0.41**	**0.73**	**0.53**

[9] Theiler. "Absorptive weak plume detection on Gaussian and non-Gaussian background clutter". In: *IEEE JSTAEORS* (2021).

[10] Guanter et al. "Mapping methane point emissions with the PRISMA spaceborne imaging spectrometer". In: *Remote Sensing of Environment* (2021).

[11] Ouerghi et al. "Model Adjusted Generalized Tests for methane plume detection on hyperspectral images". In: *WHISPERS*. IEEE. 2023.

Outline

What does the satellite see?

Derived from Beer-Lambert law

$$I = \int_{B12} a(\lambda)s(\lambda)e^{-\gamma \sum_{i=1}^{\ell} A_i(\lambda)L_i} e^{-\gamma A_{CH4}(\lambda)L_{em}} d\lambda \tag{3}$$

Notations and assumptions

- Known spectral sensitivity s of the satellite;
- Optical path $\gamma = \frac{1}{\cos\theta_{sun}} + \frac{1}{\cos\theta_{sat}}$;
- Angle of the satellite θ_{sat};
- Albedo $a(\lambda)$ of the scene constant for a given band.

Absorption spectrum

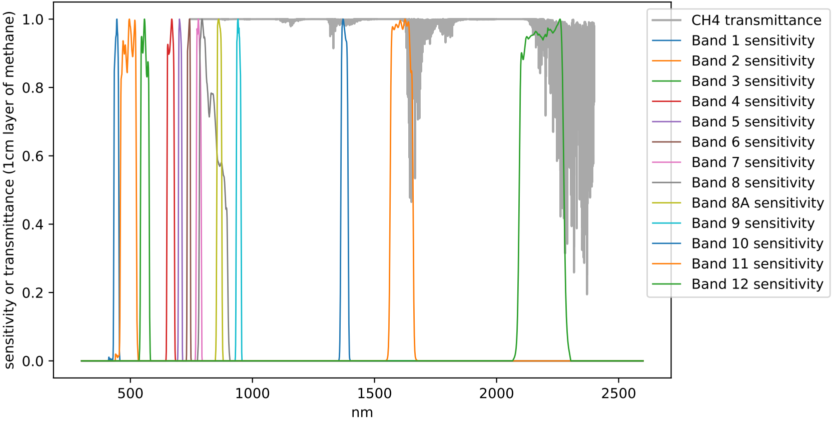

Figure 12: Methane transmittance spectrum for 1cm of methane, in gray, and Sentinel-2A spectral sensitivity for all its bands

Quantification model

Quantification (simplified atmosphere model)

$$\underset{L_{em}}{\arg\min} \left\| \frac{I_{em}}{I_{bg}} - \frac{\int_{B12} s(\lambda) e^{-\gamma A_{CH4}(\lambda)(L_{em}+L_{atm})} d\lambda}{\int_{B12} s(\lambda) e^{-\gamma A_{CH4}(\lambda) L_{atm}} d\lambda} \right\|_2^2 . \tag{4}$$

Background model[12]

$$I_{bg} = \sum_{i=0}^{t-1} w_i I_i \quad \text{s.t.} \quad \{w_i\} = \min_{\{w_i\}} \left\| I_t - \sum_{i=0}^{t-1} w_i I_i \right\|^2 . \tag{5}$$

[12] Ehret et al. "Automatic Methane Plume Quantification Using Sentinel-2 Time Series". In: *IGARSS 2022-2022 IEEE International Geoscience and Remote Sensing Symposium*. IEEE. 2022, pp. 1955–1958.

Importance of the temporal dimension

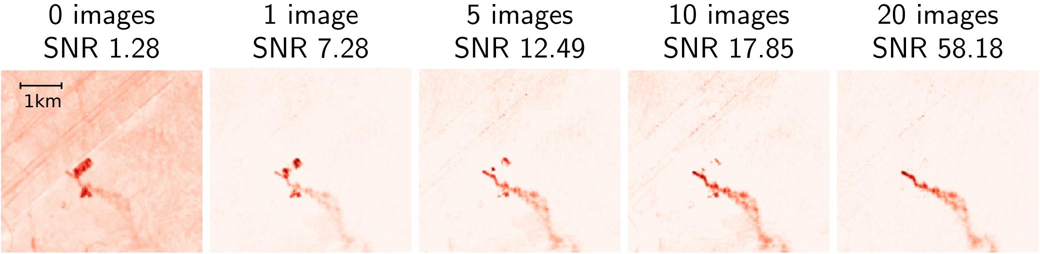

Figure 13: Impact of the number of images used during the background estimation.

Global statistics[15]

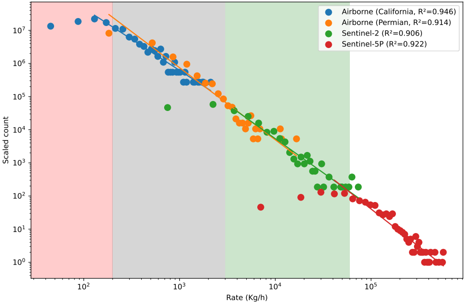

Figure 14: Power law plot of *Sentinel-5P* and *Sentinel-2* events, together with airborne campaigns over California[13] and the Permian[14].

[13] Duren et al. "California's methane super-emitters". In: *Nature* (2019).

[14] Cusworth et al. "Intermittency of Large Methane Emitters in the Permian Basin". In: *Environmental Science & Technology Letters* (2021).

[15] Ehret et al. "Global tracking and quantification of oil and gas methane emissions from recurrent sentinel-2 imagery". In: *ES&T* (2022).

Outline

Monitoring of the same location with different devices

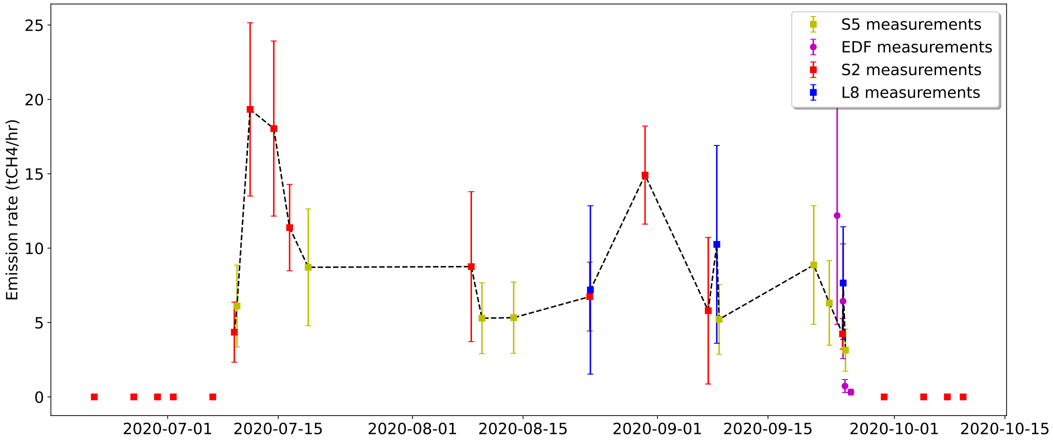

Figure 15: Emission rates measured during an event in the Permian basin occurred during the summer of 2020 (estimated latitude and longitude: 31.7335, -102.0421).

Blind studies (1)

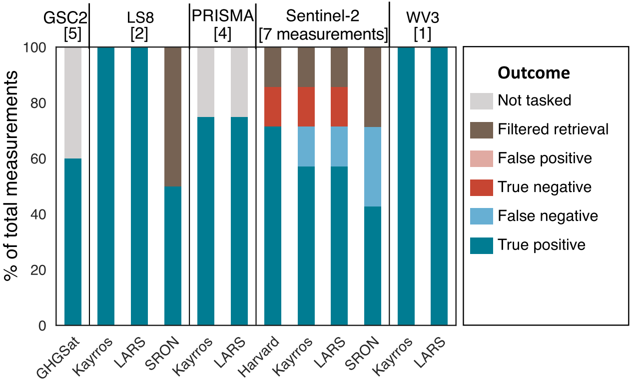

Figure 16: Detection performance by satellite and team. (source[16])

[16] Sherwin et al. "Single-blind validation of space-based point-source detection and quantification of onshore methane emissions". In: *Scientific Reports* (2023).

Blind studies (2)

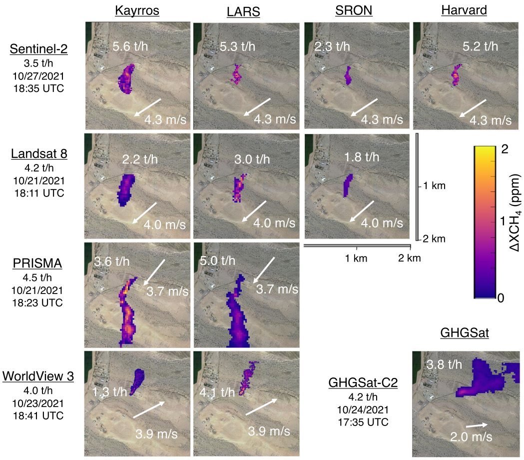

Figure 17: Examples of detected plumes. (source[13])

Outline

Global monitoring: Kayrros methane watch

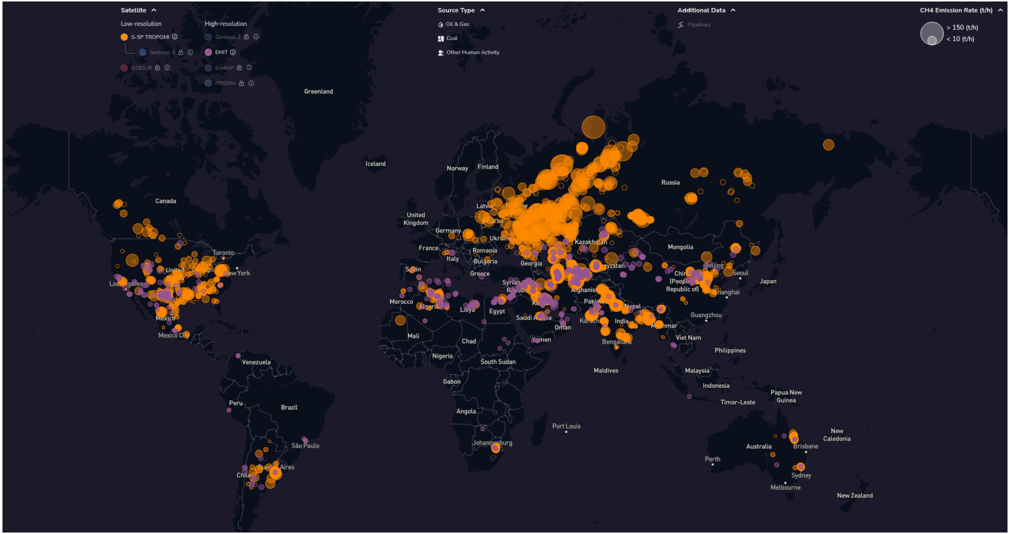

New satellites: Geostationary meteorological satellites

- Poor spatial resolution ($\sim$ 1km)
- Poor spectral resolution (similar to Sentinel-2)
- Amazing temporal resolution (1 image every 5min)
- Complete Earth coverage (GOES-R, MTG, Himawari)

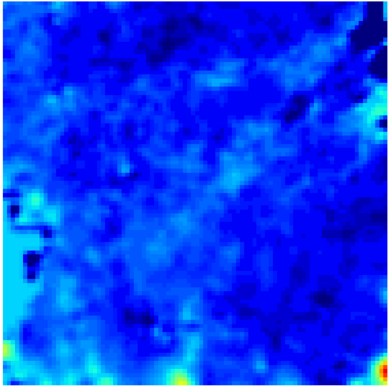

Automatic detections (1)

Deep learning[17]

- U-net architecture
- Takes as input the MF, MA-GLRT or multispectral enhancement map

Challenges

- Difficulty of annotations
- Uncalibrated data
- Limited data
- Rare events

[17] Groshenry et al. "Detecting Methane Plumes using PRISMA: Deep Learning Model and Data Augmentation". In: *NeurIPS (Workshop)*. 2022.

Automatic detections (2)

	Recall	Precision	F1
MAGLRT[18]	0.41	0.73	0.53
DCNN[19]	0.47	0.24	0.32
MF+DCNN	0.48	0.55	0.51
MAMF+DCNN	0.47	0.66	0.55
GLRT+DCNN	**0.66**	0.55	0.60
MA-GLRT+DCNN	0.56	**0.89**	**0.69**

[18] Ouerghi et al. "Model Adjusted Generalized Tests for methane plume detection on hyperspectral images". In: *WHISPERS*. IEEE. 2023.

[19] Groshenry et al. "Detecting Methane Plumes using PRISMA: Deep Learning Model and Data Augmentation". In: *NeurIPS (Workshop)*. 2022.